Radio and Coronagraph Observations: Shocks, Coronal Mass Ejections and Particle Acceleration

Monique Pick

URA CNRS 2080, DASOP, Observatoire de Paris, Meudon, 92195
E-mail: pick@obspm.fr

Abstract

Study of radio emissions which are due to accelerated electrons can provide important diagnostics on various problems. This review focuses mainly on the contribution of radio observations obtained at meter and longer wavelengths to the present knowledge of Coronal Mass Ejections (CMEs). The three main topics which are discussed in this review are the production of shocks as revealed by type II bursts and their relationship with flare-CME events, the onset and development of CMEs and finally the particle acceleration and the association with flare-CME events.

An important question which is discussed is how the recent observations support the idea that coronal and interplanetary type II bursts are of independent origin.

In the absence of a flare, past studies had found a close spatial and temporal relationship between noise storm enhancements and white light transient activity. Recent observations show that the spatio temporal evolution of noise storms in relationship with magnetic, XUV and coronagraph observations are deeply interesting for the understanding of coronal evolution.

For flare-CME events, the observations show a clear connection between radio burst emission and CME development. One can identify successive sequences in the evolution of the transient coronal activity associated with the CME development. It is emphasized that the association between CMEs, flares and accelerated particles is far from being fully understood. Observational evidence for long term coronal acceleration process is shown in this review. It is also discussed that a CME can be associated with several coronal sites of particle acceleration which are distributed over a wide volume. CMEs can also contribute to the fast particle transport from the acceleration sites to the interplanetary medium. These results agree with the fact that SEP events may contain particles of coronal origin.

Key words: — Sun: activity — Sun: corona — Interplanetary Medium

1. Introduction

Magnetic energy release in the solar corona can be produced through a large variety of dynamical processes and is closely connected to the evolution of the solar magnetic field at all spatial scales. A large amount of the energy release produces nonthermal particles accelerated either during or outside flares. Consequently, study of nonthermal radio emissions which are due to accelerated electrons can provide important diagnostics on various problems such as the dynamical behaviour and interaction of coronal structures, the relationship of transient coronal and interplanetary events and the origin of particle acceleration.

High resolution images are now available over a wide spectral range and have greatly contributed to enhance our understanding of the solar atmosphere. Radio imaging observations can be made for both limb and disk events with a higher cadence than coronagraph observations. Over the past decade, physics of Coronal Mass Ejections (CMEs) has stimulated a great deal of investigations. In particular, their relationship with flares and their potential role in the particle acceleration processes are still controversial problems. This review will focus mainly on the contribution of radio observations obtained at meter and longer wavelengths to the present knowledge of CMEs.

Radio signatures of coronal mass transients correspond in principle to both thermal and nonthermal emissions. Radio telescopes can indeed detect the additional bremsstrahlung emission due to electron-ion collision of the CME plasma. This has been reported in a few cases using meter-decameter observations obtained by Culgoora and Clark Lake instruments (Sheridan et al., 1978; Kundu and Gopalswamy 1990; Gopalswamy and Kundu, 1992; 1993). However, without polarization measurements, precise distinction between thermal and nonthermal weak emissions

may be ambiguous. In addition, nonthermal emission usually masks the thermal contribution. Flare-CME events correspond to a large variety of bursts, frequently including metric continua (type IV bursts) which cover a wide frequency range (Gosling et al., 1974). Production of shocks during flare or CMEs can be also revealed by their associated radio emission, the type II bursts, which are produced by the plasma emission mechanism at the local plasma frequency and/or at its harmonic. Finally, accelerated electron beams which propagate along magnetic field lines, excite through plasma mechanisms radio bursts which are recognized as very useful tracers of the coronal magnetic field and of its dynamical behavior. For example, type III bursts are due to electrons propagating along open magnetic lines, while type U bursts correspond to beams which travel along magnetic arches.

The three main topics which are discussed in this review are listed as follows:

- Production of shocks as revealed by type II bursts and their relationship with flare-CME events.
- Onset and development of CMEs.
- Particle acceleration and the association with flare-CME events.

2. Coronal and Interplanetary Type II Bursts

Type II radio emissions are caused by electrons accelerated by shocks at the local plasma frequency and/or at its harmonics. They are usually observed below 400 MHz (Zlobec et al., 1993). Kilometric type II radio emissions from 30 KHz to a few MHz are produced in the interplanetary medium. Two types of shocks have been invoked to explain the type II origin: the CME-driven shocks associated with rising ejecta and the blast wave shocks initiated during the impulsive phase of a flare. Thus the relationship between type II bursts and shocks is rather complex, in particular in the corona where flares and CMEs often occur conjointly. Furthermore, there exists more and more observational evidence that coronal and interplanetary (IP) type II bursts can be produced during the same event and that multiple type II bursts can be present in the same frequency range. Finally, most of the associations between CMEs, shocks and radio bursts have been based on temporal relationships between these events. In summary, an important question to be answered is: how do the recent observations support the idea that coronal and IP type II bursts are of independent origin (Wagner and Mac Queen, 1983)?

2.1. Coronal type II bursts

The first positional information came from Clark Lake and Culgoora Radioheliograph observations. Comparison between radio and coronagraph data showed that the type II burst sources are often located well below the CME leading edge (Stewart et al., 1982; Gergely et al., 1983 ; Robinson et al., 1985; Gopalswamy and Kundu, 1991). Similar conclusions were reached recently by combining images obtained by Yohkoh and LASCO/SOHO instruments with the Nanay radioheliograph (NRH) data. LASCO is composed of three coronagraphic telescopes C1, C2 and C3 which image the corona between 1.1-3.0 $R_{\odot}$, 1.5-6.0 $R_{\odot}$, and 3.7-32 $R_{\odot}$ respectively (Brueckner et al., 1995). The NRH is a multifrequency instrument which provide images in the 435-150 MHz (Kerdraon and Delouis, 1996). The comparison between the location of the events has been performed for 5 events. Spectral observations were provided by the O'Porto-Portugal and Tremsdorf-Germany radiospectrographs.

-AUGUST 18, 1996 (Klein and al., 1997). The shock wave appears to be faster than the CME and triggers the type II emission when it encounters a streamer- like structure.

-APRIL 7, 1997 (Maia et al, 1997). The shock wave does not appear to propagate along the CME direction. Comparison with coronal structures cannot be performed as the type II location lies above the disk far from the limb.

- JULY 31, 1994 and NOVEMBER 27, 1997 (Gopalswamy et al., 1997; Vilmer et al., to be published). For both events, the type II emission appears to be triggered at the leading of a X-ray like jet coming from the flare region.

-JULY 9, 1996 (Dryer et al., 1998; Pick et al., 1998). The II type burst disappeared below 80 MHz. The projected speed of the CME leading edge, about 450 km/s, is lower than the projected type II velocity which is roughly 1000 km/s. The radio source is composed of two components. One is probably located in a discrete coronal feature identified in the images of the C1 LASCO coronagraph; no coronal structure can be associated with the other component, but the formation of a thin streamer is observed at the same latitude after the coronal transient. This reveals a restructuring of the corona probably due to the passage of the shock.

2.2. Interplanetary type II bursts

The first detection of interplanetary type II bursts was made with the IMP-6 satellite at frequencies from 1850 to 292 kHz (about 14 to 37 solar radii), (Malitson et al., 1973). Their general properties were established by Cane et al.,

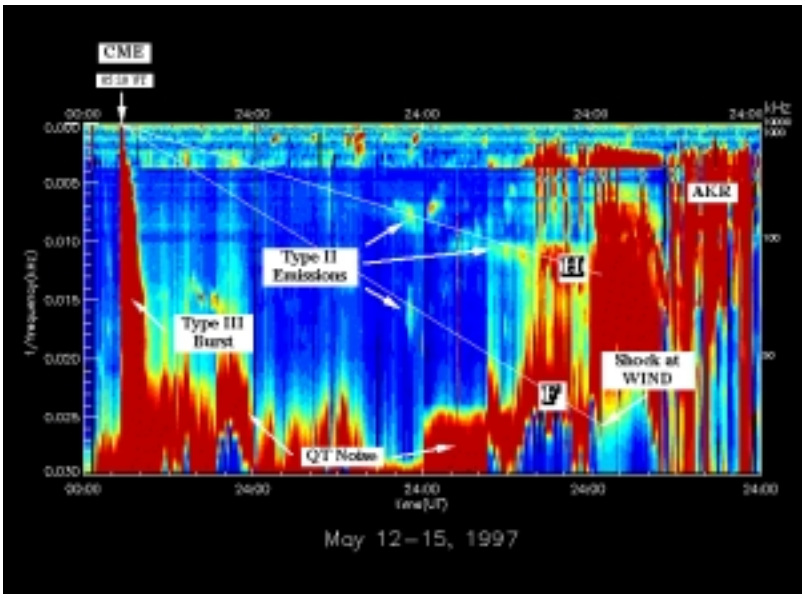

Fig. 1.. Dynamic spectrum of the Wind/WAVES radio data for the period of May 12-15, 1997 in the frequency range from 27 kHz to 13.825 MHz. The ordinate scale is the inverse of the observing frequency. The dynamic spectrum was purposely over exposed to bring out the very weak type II radio emissions. The observed weak type II radio emissions for this event lie along straight lines, labeled F and H, that originate from the CME solar lift-off time of 05:10 UT on May 12. These radio emissions are generated up stream of the CME-driven shock at the fundamental and harmonic of the plasma frequency. (From Reiner et al., 1998)

(1982). Then, it was shown that kilometric type II radio bursts were systematically associated with interplanetary shocks (Cane, 1985) and finally that all interplanetary shocks which generate kilometric type II radio bursts were associated with Interplanetary Coronal Mass Ejecta (ICMEs) (Cane et al., 1987). These ICMEs were the fastest ones.

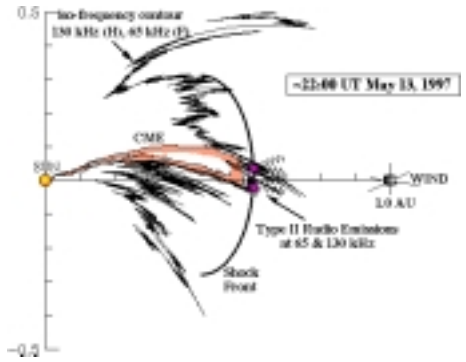

Fig. 2.. View from above the ecliptic plane at 22 :00 UT on May 13, 1997 showing the locations of the CME, the shock and the iso-frequency contour corresponding to fundamental (harmonic) type II radio emission at 64 kHz (128 kHz). The isofrequency contour was constructed by extrapolating the corotational interplanetary structures back along the Archimedean spiral determined from the measured solar wind speed and plasma density, assuming that the plasma density varies asR^{-2}. The type II radiation is expected to originate where the shock intersects this isofrequency contour. (From Reiner et al., 1998).

It is usually believed that IP type II bursts are produced by electrons accelerated in discrete sites along the ICME driven shock-front (Cane and Stone, 1984; Kahler et al., 1989). Recently, Reiner et al, (1998) proposed a new method for analyzing and tracking type II radio emissions associated with ICMEs. This method allows us to determine if the type II radio emissions occur at the fundamental and/or at the harmonic of the local plasma frequency in the upstream, or downstream, regions of the ICME driven shocks. This method has been applied to several events

detected by the WAVE radio experiment (Bougeret et al., 1995) on the WIND spacecraft. It consists in plotting the radio intensity in the dynamic spectrum versus 1/f, where f is the frequency. As the interplanetary density varies as R^{-2}, R being the radial distance from the sun, the plasma frequency fp, which is proportional to the square root of the plasma density, must vary as R^{-1}. This means that 1/f versus time will vary as R. Assuming a shock travelling with a constant velocity v, type II radio emissions will be expected to be organized as a straight line since R=v(t-t_0), t_0 being the lift-off time. The slope (= v/sqrt(a$n_0$$R_0$), n_0 being the density at R_0= 1AU) will vary as the shock speed and will be inversely proportional to the square root of the plasma density measured at 1AU; a = 9 or 18 for respectively the fundamental or the harmonic depending on the plasma frequency. This method of analysis is illustrated in Figure 1 which shows the dynamical spectrum of the type II bursts observed during the May 12-15 1997 period. A CME was observed by LASCO on May 12. The CME-driven shock arrived at WIND on May 15 as indicated in Figure 1. The signature of this shock is a sudden increase in the local plasma density. The type II radio emissions related to this event lie along two straight lines labeled F and H. The F emission is organized along a straight line going from the solar lift-off time to the measured plasma frequency upstream of the shock. Moreover, it was shown that the type II radiation appears to originate in regions along the shock front which have a density higher than the surrounding medium. This result is illustrated in Figure 2. This figure (Reiner et al., 1998) shows the location of the ICME, the shock and the iso-frequency contour corresponding to fundamental (harmonic) type II emission at 65 kHz (130 kHz). The isofrequency contour was constructed by extrapolating the corotating interplanetary structures back along the Parker spiral determined from the measured solar wind parameters. From the measured shock time at WIND, the shock transit speed was estimated and location of the CME-driven shock was deduced at the time when the radio emissions were observed at 130 kHz. The type II emission is expected to originate from the place where the shock intersects the isofrequency contour.

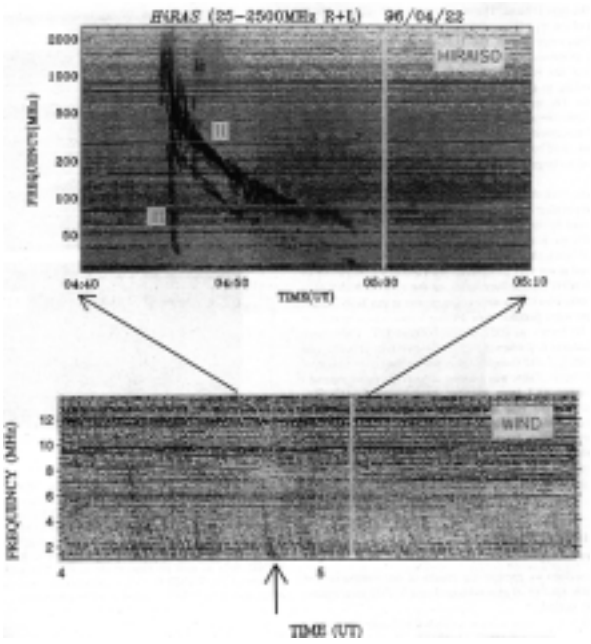

Fig. 3.. Dynamic spectrum of April 22, 1996 event from (top) Hiraiso and (bottom) WIND/WAVES. The WIND/WAVES spectrum is shown over a larger time range and the interval corresponding to the Hiraiso dynamic spectrum is indicated by the arrows. The type III burst (marked III) also starts very close to the type II onset. The bursts extend down to about 25 MHz, although there are some breaks in the type II record. The ground-based data are from the Hiraiso Solar terrestrial Research Center. In the WIND spectrum, all we see is the continuation of the main type III burst in the Hiraiso spectrum (indicated by the vertical arrow) with an additional weak type III burst before 05:00 UT. (From Gopalswamy et al., Paper I, 1998).

2.3. Do CME-driven shocks excite type II radiation in the corona?

The synthesis presented in the preceding section agrees with former ideas that coronal and interplanetary shocks have independent origins. This raises the question of whether CME-driven shocks could excite meter type II radiation

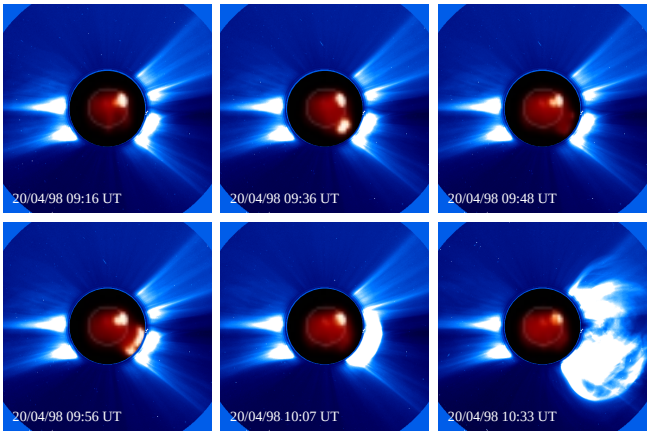

Fig. 4.. The April 20, 1998 event. Successive composites of NRH images at 164 MHz and Coronagraph C2 images showing the CME development. (A weak noise storm source is observed in the northern hemisphere). In the southern hemisphere, the onset of the radio emission is at 09:36 UT. Both the radio emission and the CME exhibit a sudden latitudinal extent at 09:56 UT and 10:07 UT respectively.

in the corona. This point was already stated in various publications and discussed in four recent studies (Gopalswamy et al., 1998 I; Gopalswamy et al., 1998.II; referred as I and II hereafter; Cliver et al., 1998; Cliver, 1998). In I, counterparts of 34 metric type II bursts were searched in the data of the WAVES instrument which covers radio frequencies below 14 MHz. One example is given in Figure 3. None of them was observed by WIND and it was concluded that most of metric type II bursts ended before reaching 14 MHz. Conversely, no correlation with coronal type II bursts was found for the 3 IP shocks of solar coronal origin observed during the same period. The authors concluded that these results are consistent with the existence of two independent types of shocks. This conclusion was criticized by Cliver (1998) who has proposed that both coronal and interplanetary shocks can be driven by a single agent, the fast CMEs (Cliver et al., 1998). In fact, this explanation is not totally contradictory to the conclusions made in I and II where it is proposed that the metric type II bursts could be triggered by short-lived drivers, the X-ray ejecta.

It may be pointed out that even if observational evidence support the concept of two shocks of independent origin, an overlap between the two kinds of type II bursts cannot be, however, excluded. For example, Kaiser et al. (1998) reported that coronal and IP type II bursts were observed in the same 1-14 MHz frequency range for one event. Furthermore, the altitude where the CME shock is formed varies and one can wonder if flare-CME events which often propagate with a constant and fast speed at low altitudes could drive coronal shocks. Data analysis of some recent events observed by the NRH and LASCO answers positively to this question.

On April 20, 1998, a CME was observed on the west limb of the sun and was associated with an IP type II burst and a shock detected at the earth by WIND. The event was partly occulted. No Hα flare was observed and the NRH observed in the southern west hemisphere a very weak radio emission (about 30 solar flux units or less) in the 410-164 MHz range. The detection of this emission was made possible because the radio sun was very quiet on this day. The most intense radio emission was probably occulted. Figure (4) represents successive composites of NRH and C2 images showing the CME in progress (a weak radio noise storm source is observed in the north hemisphere). In the southern hemisphere, the onset of the radio emission is at 09:36 UT and the flux evolution is sporadic. Both the radio source and the CME exhibit a sudden latitudinal extent at 09:56 UT and at 10:07 UT respectively. Their shape and temporal evolution are similar. We interpret this observation as an evidence for shock formation in the corona at the leading edge of the CME.

On May 02 1998, a complex radio burst was observed on the disk and was associated with a flare-CME event. A halo CME was observed for this event. Type II bursts were observed at decameter wavelengths and also in the interplanetary medium. Figure (5) shows composite images from the LASCO C2 coronagraph and from the NRH at

236 MHz. The radio image at 13:41:18 UT has been superimposed on two successive images of LASCO. At 14:06 UT, the CME has not yet reached the C2 field of view. The first available image shows that the CME was at 15:03 UT. During the interval 13:41-13:46 UT, several moving sources of short duration and spatially separated were detected. The projected speed of the eastern source displayed in Figure (5) is 1000 km/s. Fast drifting frequency emissions (estimated velocity greater than 1000 km/s) were detected by the Zurich ETH radiospectrograph during the same time interval (Pick et al., 1998). Some of these emissions could be associated with the CME-driven shock. In that case, the source motions which are detected at one given frequency could be explained by the inhomogeneity of the corona, the emission (fundamental or harmonic) coming from a volume with an extended altitude (Roelof and Pick, 1989). Alternatively, these moving sources could correspond to plasmoids.

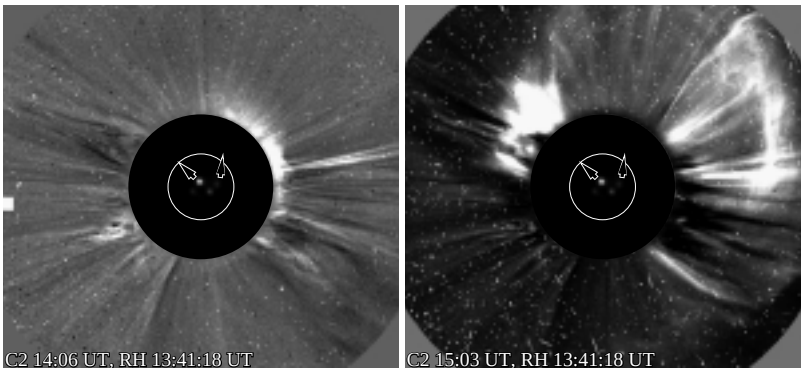

Fig. 5.. The May 2, 1998 event. Composite images from LASCO coronagraph C2 and from the NRH at 236 MHz. The radio image at 13:41:18 UT has been superimposed on two successive images of LASCO. At 14:06 UT, the CME has not yet reached the C2 field of view. The first available image showing the CME is at 15:03 UT. Several moving sources of short duration and spatially separated are detected within the same time interval. The projected speed of the eastern source is 1000 km/s.

3. Onset and Development of Coronal Mass Ejections

3.1. Radio activity and dynamical evolution of the corona in the absence of a flare

Metric activity is often observed in association with fast and slow CMEs (e.g. Gopalswamy and Kundu, 1994). Noise storms which are the most common form of activity at meter wavelengths are produced by suprathermal electrons accelerated continuously over time scales of hours or days. In addition, observation of the source evolution suggests the presence of multiple sites of energy release within the same region (Malik and Mercier, 1996). In the absence of a flare, a close spatial and temporal relationship was established between noise storm enhancements and white light transient activity (Lantos et al., 1981, Kerdraon et al., 1983). They were found to be associated with CMEs or with the appearance of additional material in the corona at the vicinity of the radio emitting source. Recent results have confirmed that the noise storm evolution appears to be well connected to the dynamical behaviour of the coronal magnetic field:

- Simultaneous observations provided by the Very Large Array (VLA) and the NRH have found the onset of a noise storm in close coincidence with the appearance of a new source at centimeter wavelengths (Raulin and Klein,1994). This has been interpreted, in agreement with former studies (Stewart et al., 1986), as evidence of an emerging magnetic flux interacting with the overlying large scale magnetic structure.

- The study of a noise storm (Bogod et al., 1985) which persisted over several days was made at different frequencies (Klein, 1997). Figure 6 shows the position of the sources superimposed on images provided by the Yohkoh Soft X-ray Telescope (SXT). The disappearance of the radio source at one frequency is seen to correspond to a shift of the emission toward lower frequencies. This observation was interpreted as evidence for a loop expansion (Klein, 1997).

- VLA observations at 400 cm and 91 cm were used to study the spatial and temporal variation of nonthermal radio bursts during CME activity detected by the SOHO instruments and by the Mauna Loa Mark III coronagraph (Habbal et al., 1996). It was noticed that the disappearance of a noise storm center followed the occurrence of a CME in the same region. Figure 7 illustrates this result. On this figure, La, Lb, Lc, Ld correspond to the positions of the noise storm centers. Disappearance of Lc between April 10 and 11 coincides with a CME development at the

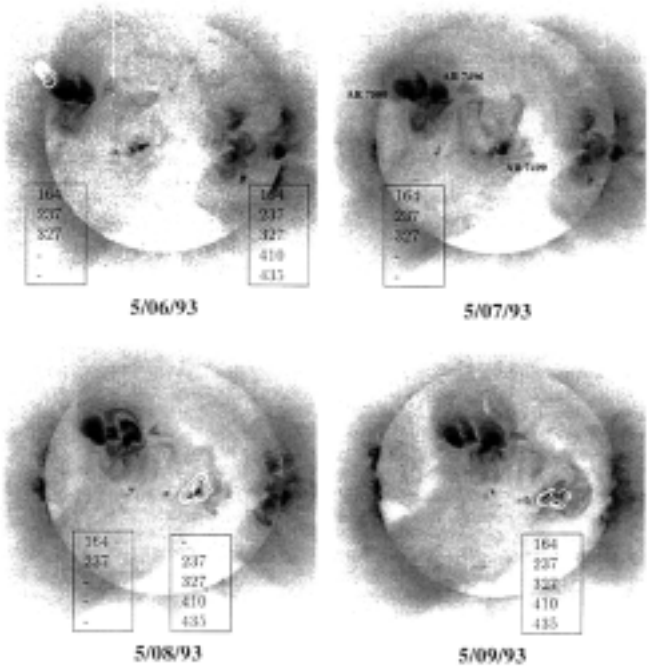

Fig. 6.. Contour of equal brightness of noise storm emission observed with the VLA at 327 MHz (91 cm), superimposed upon Yohkoh soft X-ray images of the corona on four consecutive days (Bogod et al., 1995). The inserted frames give the frequencies at which the noise storms are seen by the Nanay Radioheliograph from about 9 to 15 UT each day. No VLA observations are available on May 7. (From Klein, 1997).

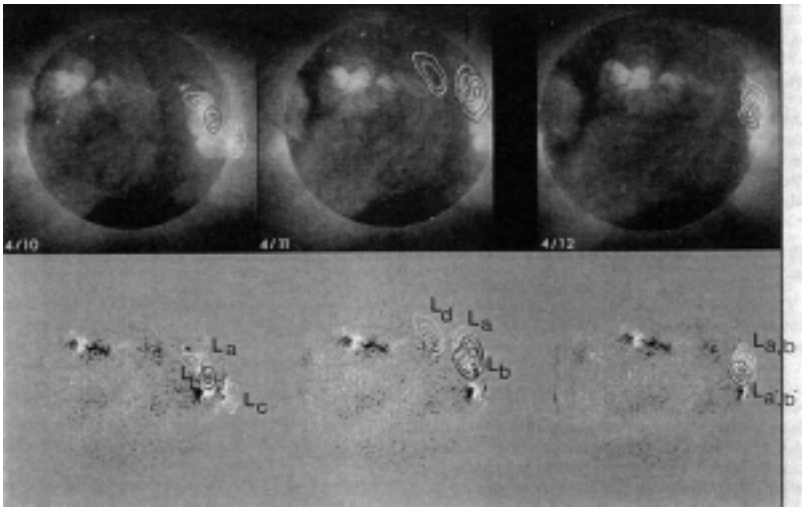

Fig. 7.. Contours of the 20 cm emission from April 10-12, 1993, superposed on the (top) X ray emission, and the (bottom) corresponding magnetograms, where black refers to negative polarity, white to positive. On each day the data were split into two halves. On April 12, there were two different pointings for the radio observations, Sun Center, and N0W35. (From Habbal et al., 1996)

.

same latitude. Similarly, disappearance of Ld between April 11 and 12 coincides with another CME also at the same latitude.

In conclusion, these studies which have been made on a few individual events show the necessity of using simultaneous spatial and temporal observations for understanding the coronal evolution over a local or more global scale.

3.2. Triggering and Development of Flare-CME events

From former studies, the association between flare-CME events and radio bursts is known to be complex involving a wide variety of physical processes. Nonthermal continua of long duration are often observed. The images obtained show that their emitting sources have often the shape of large loops or arch structure. These radio sources and the white light CME show a good correspondence with similar latitudinal extent (Gopalswamy and Kundu, 1992, 1993).

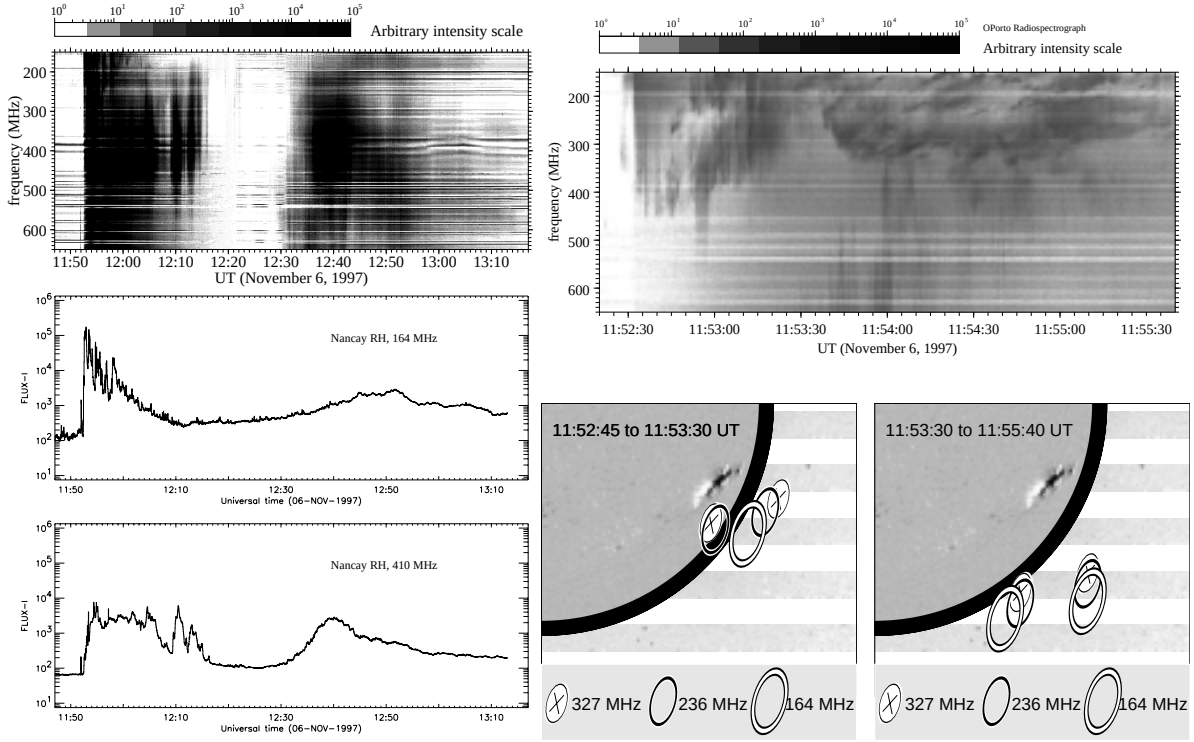

Fig. 8.. The November 6 event. *left side*: time history of the radio emission; the upper panel shows the dynamic spectrum obtained by the OPorto radiospectrograph; the lower panel are flux plots at two discrete frequencies obtained by the NRH. *Right side*: the upper panel shows a drifting frequency emission during the time interval 11:52:50 UT-11:53:30 UT; the lower panel shows that the corresponding emitting source looks like an expanding loop as revealed by the burst positions traced at distinct frequencies. (from Maia et al., 1998).

The launch of the SOHO mission has allowed us to take the advantage of the LASCO capabilities; in particular C1 is a spectroscopic coronagraph observing the "green" and "red" lines. At radio frequencies, except for the first observations of one CME made at 400 cm at the VLA (Willson et al., 1998), all the radio images at meter wavelengths were obtained with the NRH. It was found that the fast imaging and multifrequency capabilities of this instrument are of major importance in the understanding of the CME formation (Maia et al., 1998 a and b; Pick et al., 1998). The main results can be summarized as follows:

-During the rapid development of the event, the radio signatures of the initial instability usually correspond to type III or U bursts of short duration. This triggering effect takes place in a small volume located near the flaring active region and probably results from the interaction between two magnetic loops.

-Successive sequences, in the evolution of the coronal restructuring, leading to the full latitudinal extent of the CME, can be identified. Identification and timing of these sequences result from the analysis of the radio emission. Multipolar magnetic systems are involved in the CME development, as also suggested by Webb et al. (1997) and shown by Dere et al (1997). Spatial and temporal evolution of the radio sources strongly suggest that the full

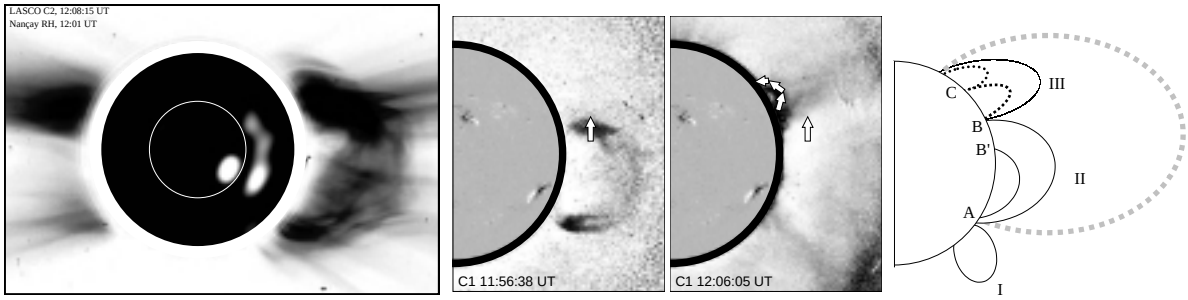

Fig. 9.. The November 6 event From left to right side:- Composite image of one C2 image with one radio image at 164 MHz.- FeX image which shows the evolution of the CME seen in C1; the arrows indicate the distribution in the northern hemisphere of the emitting components observed at 164 MHz before 12:00 UT (left) and after 12:00 UT (right)- Sketch of the successive coronal loops involved in the CME development; A, B, and C correspond to regions where two adjacent loops are interacting together. (from Maia et al., 1998)

latitudinal extent of the CMEs is reached within the first minutes.

These results are illustrated on Figures 8 and 9 which display the main steps in the evolution of the CME observed on November 6, 1997 (Maia et al., 1998). The C1 Fe X and XIV images show loops between regions labeled A and B' and A and B after 11:52 UT as displayed in Figure 9. Figure 9 (right side) is a sketch of the successive coronal structures involved in the development. The loop which connects A and B is expanding. The first available image in C2 shows that at 12:08:15 UT the CME is already halfway through the C2 field of view. Figure 8 displays the spectral evolution of the radio emission and the flux at two discrete frequencies (left side). Two parts can be distinguished: the first one before 12:25 UT is characterized by an outburst with rapid fluctuations superimposed on a continuum; the second one is a continuum enhancement. After a group of short bursts, the outburst develops very rapidly. Between 11:52:50 UT and 11:53 :40 UT, the spectrum shows an emission which drifts from 430 MHz to 200 MHz. This is displayed in Figure 8, right side. Figure 8 displays also the positions of the sources at distinct frequencies. They trace a loop-like structure which expands with a velocity of the order of 3000 km/s , labeled I in the sketch of Figure 7. A second loop is detected at 11:50:00 UT. The counterparts of the two successive loops were identified in C2 images. At the onset of the continuum, around 11:54:30 UT the source evolution becomes more complex. The radio emission from the southern hemisphere consists of several components with a large concentration above region A and also some of them above B. New intermittent sources appear in the northern hemisphere first in B then in C. Region C and streamers overlap as shown in the middle part of Figure 8. At the lowest frequencies of the NRH an extended region is observed firstly at 236 MHz then later at 164 MHz as shown in Figure 8, left side. C2 images show that the CME overlies the radio source precisely and has the same latitudinal extent. The radio emission corresponds to rising loops and a drift in the continuum emission is seen in the spectrograph data. The space time history of the radio emission reveals the existence of successive regions of interaction A, B then C between two adjacent expanding loops. The appearance of region C is consistent with the modification of the FeX image seen in the same region and the opening of the structure also seen in FeX (Figure 8, middle part). In the second part of the event, the emitting source is concentrated in region A. This site coincides with post flare loops. In conclusion the comparison of radio and coronal observations show that the CME results from multiple loop interactions. The latitudinal extent of the CME reaches 100° within about four minutes.

4. Particle Acceleration and the Association with CME-Flares Events

The association between CMEs, flares and accelerated particles is far from being fully understood. It has been widely reported that the large solar energetic particle events (SEP) are associated with shock waves driven out from the Sun by CMEs (e.g. Reames, 1995). In fact, the problem is much more complex than what is expressed sometimes with authority in the literature. A detailed discussion on this topics is beyond the scope of this paper. One can, however, recall a few points :

-X-ray and radio observations have given evidence for long term acceleration in the corona on time scales of hours or more for subrelativistic electrons (e.g. Pick, 1986) . This was also shown for relativistic ions above some tens of MeV (Leikov et al., 1993; Kocharov et al., 1994, Akimov et al., 1996) and recently for protons of tens to hundreds

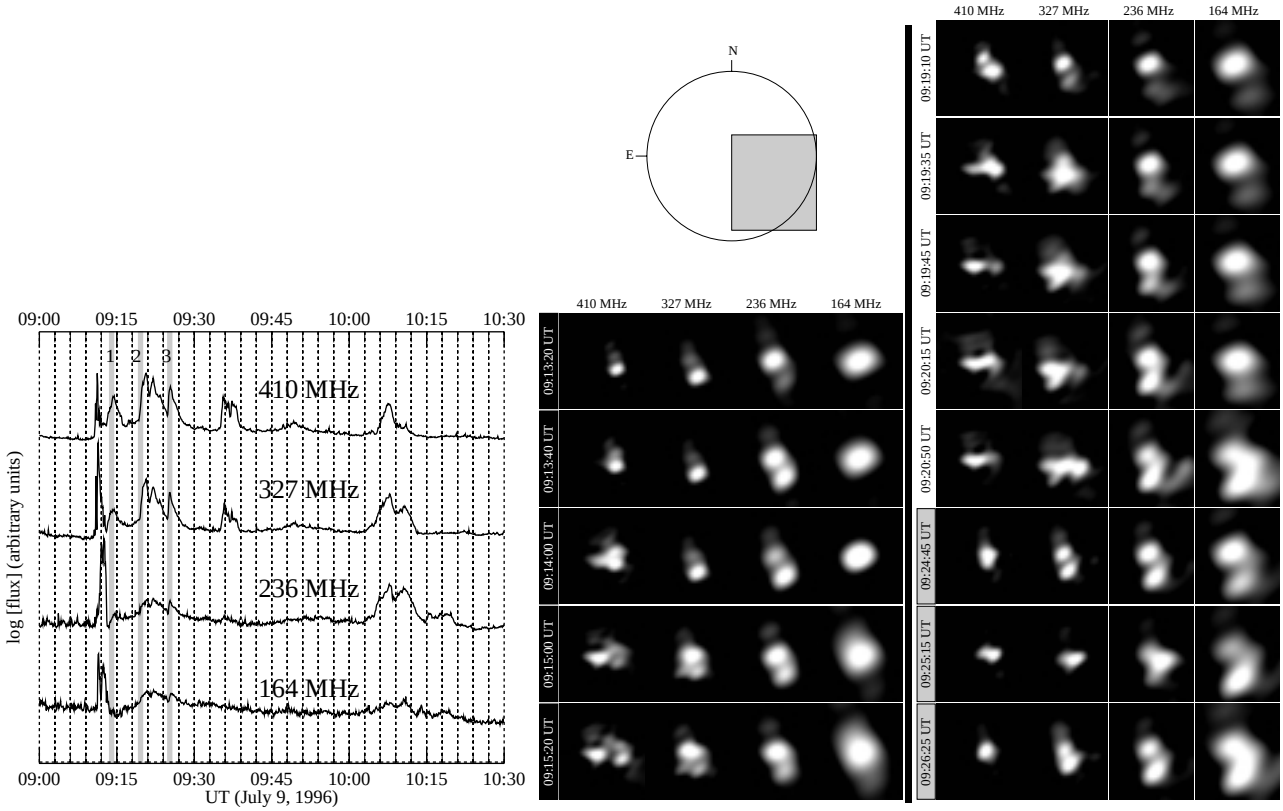

Fig. 10.. The July 9 1996 event. *Left panel*: time evolution of the radio flux at distinct frequencies ; the grey bars correspond to selected periods for which the spatial maps of successive emitting radio sources are displayed in the right panel. *Right panel*: spatial evolution of the successive radio-emitting sources observed at all frequencies during the development of the radio continuum after 09 :12 UT. The selected period are indicated in Figure 10 by grey bars. (From Pick et al., 1998).

of MeV by Klein et al., (1999) who also inferred a relationship between the time evolutions of coronal acceleration and of protons fluxes at 1 AU.

-There is some evidence that SEP events may contain both particles from solar flares and from CME-shock origin (Cliver, 1995).

-The Ulysses mission has given the opportunity to investigate the particle transport in latitude, i. e. in a physical situation simpler than that one met in the study of longitudinal transport near the ecliptic plane where the magnetic field is very complex. It was shown that accelerated particles of coronal origin can be channeled inside CMEs (Armstrong et al., 1994; Pick et al., 1995 a,b) and that the CMEs might play an important role in the particle transport.

-Particles of solar origin were detected at high latitudes, far from the associated active region (Pick et al., 1995,c). It was proposed that a large scale restructuring of the corona built up the conditions for a fast particle transport from low to high latitudes (Manoharan et al., 1996; Buttighoffer et al.,1996). During CMEs the opening of the large scale coronal structures (as shown in the preceding section) provides the coronal particles with an access to the interplanetary medium. These particles can promptly spread over a large range of heliolongitude and latitude (Pick et al., 1998; Maia et al., 1998). In addition, electron acceleration is not restricted to the flare region but involves a large volume of the corona. For example, during the November 6, 1997 event, at least three accelerating coronal sites (A, B and C) have been identified.

-Observational evidence for long term coronal acceleration process is illustrated in Figure 10. On 9 July 1996, the NRH observed a radioburst on the disk associated with a flare-CME event initiated in an active region located at S10° W30°. The time evolution of this burst is reported in Figure 10, left panel. One can distinguish two sequences: the first one which takes end at about 09:13 UT corresponds to an outburst; the second one corresponds

to the progressive development of a long duration continuum observed on the whole spectral range of the NRH.This continuum exhibits two major series of several sudden flux enhancements at all frequencies. Figure 10, right panel, displays the spatio-temporal evolution of the emitting region with an integration time of 5s during selected periods indicated by thick grey bars and numbers in Figure 10. The source structure is first of all composed of two components which remain detectable until the end of the event. While the northern component remains at the same position above the active region, a progressive displacement of the southern component is observed. Furthermore in coincidence with each sudden flux enhancement, the structure of the source exhibits a strong modification which is observed at all frequencies. This modification is characterized by the appearance of a new component located in between the two preexisting components with an east-west orientation roughly perpendicular to the former structure. During enhancement 1, this component appears first at 410 MHz then at 327 MHz. This is immediately followed by a strong change of the emitting region at these two frequencies. The same scenario repeats itself at each enhancement. The topology and the evolution of the emitting sources strongly suggest successive interactions between rising arches and other loops (for more details, see the paper, Pick et al., 1998). Furthermore, these observations strongly suggest that the electrons responsible for the flux enhancements are the result of these interactions. This result is consistent with a continuous electron acceleration process over a long time period rather than a long-term electron coronal storage.

5. Concluding Remarks

Most of the important results emerged from coordinated studies between radio observations and data obtained in others spectral domains. Some of the results were derived from the study of individual events and the conclusions are still preliminary. Furthermore, comparisons with coronal data in particular, are often limited by the cadence of the coronagraph observations. Despite of these limitations, several results presented here are very promising:

-Study of the spatio temporal evolution of noise storms in relationship with magnetic, XUV and coronagraph observations are deeply interesting for the understanding of coronal evolution.

-Several points on the origin of metric type II bursts need still to be clarified.

Recent measurements which have been made at higher frequencies than the former ones have confirmed that the positions of metric type II bursts and of the leading edges of CMEs most often do not coincide. No propagation effect or ionospheric refraction can account for this result.

Coronal waves are often accompanied by type II bursts (Thompson et al., 1998) but their physical link is far from being established. For example, the type II burst and the coronal wave observed during the April 7, 1997 event did not fit in time nor in position (the type II burst was observed from 13:59 to 14:02 UT at 164 MHz and south from the flare region).

The suggestion of a possible association between metric type II bursts and short-fast drivers is interesting and has to be carefully examined. In that respect, the fast expanding loop which was observed at the onset of the November 6 event, 1997 and which coincides with the fast drifting radio emission, might be the signature of a fast driver. If it is the case, let us emphasize that this fast loop contributes to the triggering of the whole event, as explained in the previous section, but is distinct from the leading edge of the CME.

-It was finally briefly summarized that in addition to the flaring site itself, a CME can be associated with several coronal sites of particle acceleration which are distributed over a wide volume. CMEs can also contribute to the fast particle transport from the acceleration sites to the interplanetary medium.

6. Acknowledgments

I acknowledge discussions with D. Maia and N. Vilmer. I am indebted to J. Bonmartin, A. Bouteille and M. Savinelli who helped me in the figure production. I am grateful to O. Malandraki for the critical reading of the manuscript.

References

Akimov et al., 1996, Solar Phys., 166, 107
Armstrong T. P. et al.,1994, Geophys. Res. Lett., 21, 17, 1747
Bogod V. M., Garigov V., Gefreikh G.B. et al., 1995, Solar Physics,111, 31
Berdichevsky and 14 coauthors, 1998, Geophys. Res. Letters, 25, 14, 2474
Bougeret J.L. et al., 1995, Space Science Rev., 71, 231

Brueckner G. E. and 14 coauthors, 1995, Solar Phys., 162, 357
Buttighoffer A, Pick, Raviart A., Hoang S., Lin R. P., Simnett G. M., Lanzerotti L. J. and Bothmer V. 1996, Astron. Astrophys., 316, 499
Cane H. V., Stone R. G., Fainberg J. F., Steinberg J. L. and Hoang S., 1982, Solar Phys., 78, 187
Cane H. V. and Stone R. G., 1984, Astrophys. J., 282, 339
Cane H. V., J. Geophys. Res., 1985, 90, 191
Cliver E. W., 1995, High Energy Solar Physics, R. Ramaty, N. Mandzhavidze and Xin-Min Hua (eds.), AIP Conf. Proc., 374, 3
Cliver E. W., 1998, , J. Geophys. Res., in press
Cane H. V., Sheeley, Jr N. R. and Howard R. A., 1987, J. Geophys. Res., 92, 9869
Dere K. P., et al., 1997, Solar Phys., 175, 601
Dryer M. and 23 coauthors, 1998, Solar Phys., 181, 159
Gergely T. E., Kundu M. R. and Hildner E., 1983, Ap. J., 268, 217
Gopalswamy N. and Kundu M., 1991, AIP Conference Proceedings 264, ed. G. P. Zank and T. K. Gaisser, 257
Gopalswamy N. and Kundu M. R., 1992, Ap. J., 390, L38
Gopalswamy N. and Kundu M., 1993, Solar Phys.,143, 327
Gopalswamy N. and 5 coauthors, 1997, Ap. J., 486, 1036
Gopalswamy N. and 8 coauthors, 1998, , J. Geophys. Res., 103, 1, 307, Paper I
Gopalswamy N. and 8 coauthors, 1998, , J. Geophys. Res., 104, 4749, Paper II
Gosling J. T., Hildner E., MacQueen R. M., Munro R. H., Poland A. I. and Ross C. L., 1974, J. Geophys. Res., 79, 31
Habbal S. R., Mossman Amy, Gonzales R. and Esser R., J. Geophys. Res., 1996, 101, A9, 19943
Kahler S. W., Cliver E. W. and Cane H. V., 1989, Solar Phys., 120, 393
Kerdraon A. and Delouis J. M., 1996, Lecture Notes in Physics Ed. G. Trottet, Springer-Verlag, Berlin, P. 192
Kerdraon A., Pick M., Trottet G. et al., 1983, Ap J, 265, L19.
Klein K. L., Klassen A., Aurass H. and LASCO consortium, 1997, Proceedings of the Fifth SOHO workshop, ESA SP 404, 461
Klein, K. L., Advances in Solar Physics, Euroconference, Three dimensional structure of solar active regions (Greece), 1997 October 7-11.
Klein K. L. and 6 coauthors, 1998, Astron. Astrophys., submitted
Kocharov L. JG., et al., 1994, Solar Phys., 150, 267
Lantos P., Kerdraon A., Rapley G. G. and Bentley R. D., 1981, Astron. Astrophys., 101, 33
Kundu M. and Gopalswamy N. , 1990, Solar Phys., 129, 133
Leikov N. G. et al., 1993, Astron. Astrophys., 97, 34
Maia D., Pick M., Howard R., Brueckner G. E. and Lamy P., Proceedings of the Fifth SOHO workshop, ESA SP 404, 539
Maia D. and 11 coauthors, 1998, Solar Phys., 181, 121
Maia D., Vourlidas A., Pick M. and Howard R., 1999, J. Geophys. Res., in press
Malik R.. K. and Mercier C., 1996, Solar Phys., 165, 347
Malitson H. H., Fainberg J. and Stone G., Astroph. Letters, 1973, 14, 111
Manoharan P. K., Van Driel-Gesztely L., Pick M. and Demoulin P., 1996, Astrophys J., 468, L73
Pick M., 1986, Solar Phys., 104, 19,
Pick M. , Buttighoffer A. et al., 1995a, Space Science Rev., 72, 315
Pick M. and 5 coauthors, 1999, Solar Wind 9 Conference, Ed. S. Habbal, in press
Pick M. et al., 1995b, Geophys. Res. Lett., 22, 3373
Pick M. et al., 1995c, Geophys. Res. Lett., 22, 3377
Pick M. and 12 coauthors, 1998, Solar Phys., 181, 455
Raulin J. P. and Klein K.L., 1994, Astron. Astrophys., 281, 556
Reames D. V., 1995, Adv. Space Res., 15, 7, 41
Reiner M. J., Kaiser M. L., Fainberg J., and Stone R. G., 1998, J. Geophys. Res., in press
Roelof E. C. and Pick M., 1989, Astron. Astrophys., 210, 417
Robinson R. D. and Stewart R. T., 1985, Solar Phys., 97, 145
Sheridan K. V., Jackson B. V., McLean D. J., and Dulk G. A., 1978, Proc. Astron. Soc. Australia, 3, 249
Stewart R. T., Dulk G. A., Sheridan K. V., House L. L., Wagner W. J., Sawyer C and Illing R., 1982, Astron. Astrophys., 216, 217
Stewart R. T., Brueckner G.E., Dere K. P., 1986, Solar Phys., 106, 107
Thompson B. J. and 9 coauthors, 1998, Astrophys. J. Letters., in press
Wagner W. J. and MacQueen R. M., 1983, Astron. Astrophys., 120, 136
Webb D. F., Kahler S. W., McIntosh P. S. and Klimchuck J. A., 1997, J. Geophys. Res., 102, A 11, 24161
Willson R. F., Redfield, Lang K. R., Thompson B. J. and St. Cyr O. C., 1998, Ap. J., 504, L117
Zlobec P. Messerotti M., Karlicky M. and Urbarz H., 1993, Solar Phys., 144, 373